

AD-A064 762

AIR FORCE INST OF TECH WRIGHT-PATTERSON AFB OHIO SCH--ETC F/6 7/2  
PURE SULFUR DISCHARGES AND ASSOCIATED SPECTRA.(U)  
OCT 78 D A PETERSON  
AFIT/SEP/PH/78D-10

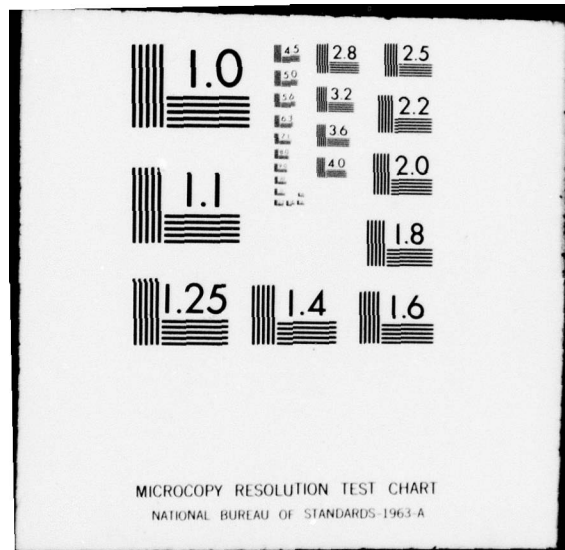
UNCLASSIFIED

NL

|OF|  
AD  
A064762



END  
DATE  
FILMED  
4 -79  
DDC



① LEVEL

ADA064762

DDC FILE COPY

PURE SULFUR DISCHARGES  
AND ASSOCIATED SPECTRA

THESIS

AFIT/GEP/PH/78D-10

Drew A. Peterson  
Capt USAF

DDC  
APPROVED  
FEB 22 1979  
A

14 AFIT/GEP/PH/78D-10

6 PURE SULFUR DISCHARGES  
AND ASSOCIATED SPECTRA

Thesis

9 Master's thesis

Presented to the Faculty of the School of Engineering  
of the Air Force Institute of Technology  
Air Training Command  
in Partial Fulfillment of the  
Requirements for the Degree of  
Master of Science

12 58 P.

ADMISSION BY	
DTIC	Write Section <input checked="" type="checkbox"/>
DDI	Mail Section <input type="checkbox"/>
CHARACTER	<input type="checkbox"/>
JUSTIFICATION	
BY	
CATEGORICAL/AVAILABILITY CODES	
Dist. STATE and/or SPECIAL	
A	

10 by Drew A. Peterson B.S.

Capt USAF

Graduate Engineering Physics

11 October 1978

Approved for public release; distribution unlimited.

012 225

elt

## Preface

The author gratefully acknowledges the efforts, support and encouragement of the many people (too numerous to identify individually) who made this study possible. Also, the support of ARTO of AFWL, the metalurgy lab and the machine shop at KAFB NM have been essential in accomplishing the work presented here. A special thanks is extended to Brenda St. James for manuscript typing, to Diana Hudson for final typing, and to Jan Marien for glassblowing and consultation; finally, to Dr. LaVerne Schlie for sponsoring and sheperding the entire project.

## Contents

	Page
Preface . . . . .	ii
List of Figures . . . . .	iv
List of Tables . . . . .	v
Abstract . . . . .	vi
I. INTRODUCTION . . . . .	1
II. ELECTRONIC STRUCTURE, DISCHARGE PHYSICS, AND MOLECULAR PROCESSES	
Physical Characteristics . . . . .	3
Discharge Physics . . . . .	7
Molecular Processes . . . . .	11
III. EXPERIMENTAL TECHNIQUE	
Description . . . . .	13
Scanning Apparatus . . . . .	16
Tube Construction . . . . .	7
IV. RESULTS AND ANALYSIS . . . . .	
Discharge Characteristics . . . . .	20
Spectra . . . . .	22
Oscillation Frequency . . . . .	26
Building Deslandres Tables . . . . .	28
Observing the S <sub>2</sub> (B-X) System . . . . .	32
V. CONCLUSIONS . . . . .	36
VI. RECOMMENDATIONS . . . . .	37
BIBLIOGRAPHY . . . . .	38
APPENDIX A . . . . .	40
APPENDIX B . . . . .	44
APPENDIX C . . . . .	45
VITA . . . . .	47

List of Figures

<u>Figure</u>		<u>Page</u>
1	Concentrations of Various Sulfur Species in Saturated Vapor, from Room Temperature to the Boiling Point . . . . .	5
1a	Total Vapor Pressure of Sulfur vs Temperature . . . . .	6a
2	Low Lying Energy Levels of Atomic Sulfur . . . . .	8
3	High Lying Energy Levels of Atomic Sulfur . . . . .	9
4	Some of the Potential Energy Curves of the S <sub>2</sub> Molecule	10
5	The Experimental Setup - Pictured Schematically . . . . .	14
6	The Actual Experimental Setup . . . . .	15
7	Voltage Current Characteristics of a Sulfur Discharge Tube . . . . .	21
8	A Strip Chart Emission Spectra of the S <sub>2</sub> Molecule . . .	24
9	Time Integrated Emission Spectra of the S <sub>2</sub> Molecule . .	25

List of Tables

<u>Table</u>		<u>Page</u>
1	The Deslandres Table of the $B^3\Sigma_u^- - X^3\Sigma_g^-$ System ( $v'' \leq 10$ ) . . . . .	29
2	The Deslandres Table of the $B^3\Sigma_u^- - X^3\Sigma_g^-$ System ( $v'' > 10$ ) . . . . .	30
3	The Deslandres Table of the $B^{11}3\Pi_u^- - X^3\Sigma_g^-$ System ( $v'' \leq 10$ ) . . . . .	34
4	The Deslandres Table of the $B^{11}3\Pi_u^- - X^3\Sigma_g^-$ System ( $v'' > 10$ ) . . . . .	35



Abstract

Stable, glow discharges in pure sulfur and He-sulfur have been achieved for the first time, at operating temperatures between  $0^{\circ}\text{C}$  and  $250^{\circ}\text{C}$ . This result indicates that  $\text{S}_8$  is broken directly into  $\text{S}_2$  and means that temperatures much less than  $600^{\circ}\text{C}$  can be used. The  $\text{S}_2$  (B-X) band emission is observed in great detail, and through analysis of these spectra the ground electronic state constants have been determined to the fourth order. The first observation of the  $\text{B}^{\prime\prime} \text{ } ^3\pi_{\text{u}}^{-} - \text{X}^3\Sigma_{\text{g}}^{-}$  system transitions is made, and tentatively identified. Only  $\text{S}_2$  band emission is observed and no atomic lines were observable.

## I. INTRODUCTION

Recently, Leone and Kosnik<sup>1</sup> demonstrated visible and u-v lasing on the bound-to-bound  $B^3\Sigma_u^- - X^3\Sigma_g^-$  transition of  $S_2$  via optical pumping. The  $S_2$  system is particularly attractive as a high efficiency, low pressure laser system because of the relative positions and well depths of the  $B^3\Sigma_u^-$  and  $X^3\Sigma_g^-$  states. The relative position of the upper and lower states are displaced such that the lowest vibrational levels of the  $B^3\Sigma_u^-$  state lie above high vibrational levels of the ground  $X^3\Sigma_g^-$  state. However, unlike other demonstrated bound-to-bound laser systems, like  $Na_2$ <sup>2</sup> and the Hg-halides<sup>3-7</sup>, the upper electronic state of  $S_2$  has a threshold excitation energy less than the dissociation energy of the ground state. Such a situation implies that for electrical excitation the  $B^3\Sigma_u^-$  state should be directly excited from the ground state and the amount of ground state dissociation via electron impact should be negligible. Under these conditions, high pressure operation ( $\geq 1$  Atm) should not be necessary, because the  $S_2$  system does not depend on high number densities to work. In theory it should work with one molecule. Such a system is directly scalable and greater number densities should yield a linear increase in power, assuming no high density destructive processes exist. The quantum efficiencies of sulfur transitions around  $4000 \text{ \AA}$  is greater than 75% and the sulfur band system is so extensive that an  $S_2$  laser should be tunable from the U-V to the visible. These energy levels also indicate the potential for high fractionally power transfer to the  $B^3\Sigma_u^-$  from the ground state.

Emission from the  $S_2$  (B-X) transitions has previously been observed easily in flames, shock tubes and electrical discharges containing sulfur

compounds<sup>8,9</sup>. The work of Lakshmenarayana and Mahajon<sup>9</sup> was the first experimental observation of the sulfur afterglow spectrum but, unfortunately, they never mentioned the temperature range, pressure range, and discharge conditions in which they worked. Leone and Kosnik<sup>2</sup> in their optical pumping experiment were forced to operate at 600°C in order to thermally dissociate the sulfur S<sub>8</sub> molecules into the necessary S<sub>2</sub> molecules.<sup>10</sup> This thesis shows that such high temperatures are not required, by presenting the first observation of the spectra from self-sustained CW and pulsed electrical discharges in pure sulfur and He/sulfur mixtures in the temperature range from 0°C to 250°C with corresponding vapor pressures of 10<sup>-5</sup> torr to 8 torr. The data show that the S<sub>8</sub> molecules are electrically dissociated into S<sub>2</sub> molecules, thus eliminating the 600°C operating temperature requirements. The discharges were stable and the only spectra observed in the spectral range from 2800-7000 Å was that of S<sub>2</sub>. Exactly the same spectra was seen in both CW and pulsed experiments. Careful analysis of the B<sup>3</sup>Σ<sub>u</sub><sup>-</sup> - X<sup>3</sup>Σ<sub>g</sub><sup>-</sup> transitions has resulted in the determination of the ground state constants out to the quartic term W<sub>e</sub>Z<sub>e</sub>. Using these data, observation and analysis of the much weaker B<sup>3</sup>Π<sub>u</sub><sup>-</sup> - X<sup>3</sup>Σ<sub>g</sub><sup>-</sup> transitions which overlap the strong B<sup>3</sup>Σ<sub>u</sub><sup>-</sup> - X<sup>3</sup>Σ<sub>g</sub><sup>-</sup> transitions have been made for the first time. The predissociative cutoff of the B<sup>3</sup>Σ<sub>u</sub><sup>-</sup> state by the previously proposed 1<sub>u</sub> state of S<sub>2</sub> is definitely observed.<sup>9</sup> In Section II, the important laser and discharge physics will be discussed and then in Section III, the details of the experimental procedure will be described. Finally, in Section IV, the results will be presented along with a detailed discussion.

## II. PHYSICAL CHARACTERISTICS AND DISCHARGE PHYSICS OF SULFUR

### A. Sulfur Physical Characteristics

Many references have described the behavior of sulfur as a solid, liquid and gas. Unfortunately though, the behavior of sulfur, particularly its molecular composition while in the vapor phase is not clearly understood<sup>10</sup>. As a vapor it is known to exist as a combination of  $S_8$ ,  $S_7$ ,  $S_6$ ,  $S_5$ ,  $S_4$ ,  $S_3$ , and  $S_2$  molecules in varying concentrations at various temperatures and pressures. At low pressures of a few torr and temperatures of about  $600^\circ\text{C}$ , the sulfur vapor is predominantly  $S_2$  molecules.<sup>10</sup> Leone and Kosnik<sup>1</sup> were forced to operate at these temperatures in order to have sufficient  $S_2$  molecules present in their optically pumped laser test cell. Under these conditions the  $S_8$  molecules are thermally dissociated. However, in this electrical excitation experiment, the electrons have energies much larger than the thermal energies required and consequently, electrical excitation of  $S_2$  molecules at lower temperatures would be strongly expected.

When solid orthorhombic sulfur is heated in a sealed evacuated tube, it first melts into a pale yellow liquid of low viscosity at about  $113^\circ\text{C}$ .<sup>10</sup> The properties of this liquid, which consists primarily of  $S_8$  molecular rings, shows no unusual behavior up to about  $159^\circ\text{C}$ . At this temperature, there is an abrupt and very large increase in its viscosity. This temperature of  $159^\circ\text{C}$  is called the transition temperature or "floor temperature". The commonly accepted explanation of this phenomenon is that at  $159^\circ\text{C}$ , and higher, the  $S_8$  rings begin to break up and form  $S_8$  chains or polymers. The theory to explain the equilibrium polymerization in sulfur between the  $S_8$  rings and  $S_8$  chains was originally done by

Powell and Eyring<sup>12</sup> in 1943 and by Gee<sup>13</sup> in 1952. These attempts were only partially successful. In 1959, Tobolsky and Eisenberg<sup>14</sup> used two equilibrium constants, one for initiation and one for the propagation of the equilibrium polymerization in sulfur. This theory has proven to be successful in describing the behavior of sulfur over its entire liquid range, including the transition region. The details of this study will not be discussed here, but its effects are particularly noticeable in the sulfur discharge's uniformity. This is especially observed in pulsed excitation experiments. It is conjectured that at temperatures below 160°C, the sulfur vapor exists as S<sub>8</sub> ring molecules and consequently acts as a large electron attaching molecule, similar to ion clustering.<sup>15</sup> Temperatures above 160°C thermally dissociate the S<sub>8</sub> rings into S<sub>8</sub> chains that have a low electron attachment cross section. During pulsed operation, once this 160°C temperature limit was exceeded, very stable glow discharges resulted via dissociation of the S<sub>8</sub> chains and formation of S<sub>2</sub> molecules.

The equilibrium composition of saturated sulfur vapor can be calculated utilizing known experimentally obtained constants. Berkowitz<sup>16</sup> calculated the partial pressures of the various molecular species using the measured equilibrium constants, the heat and free energies of formation of S<sub>2</sub> through S<sub>8</sub>, and the data of West and Menzies<sup>18</sup> for total vapor pressure. This is shown in Fig. 1. Notice that at 750°K, most of the sulfur exists as either S<sub>6</sub>, S<sub>7</sub> or S<sub>8</sub> molecules and less than 3% of S<sub>2</sub> at 480°C (750°K). Braune, Peter and Neveling<sup>19</sup> have experimentally determined that at 600°C approximately 80% of the sulfur molecules exist as S<sub>2</sub> molecules. A temperature of 600°C corresponds to .075 eV, an energy very easily acquired from the discharge electrons. Thus, the electrical dissociation of S<sub>8</sub> through S<sub>3</sub>

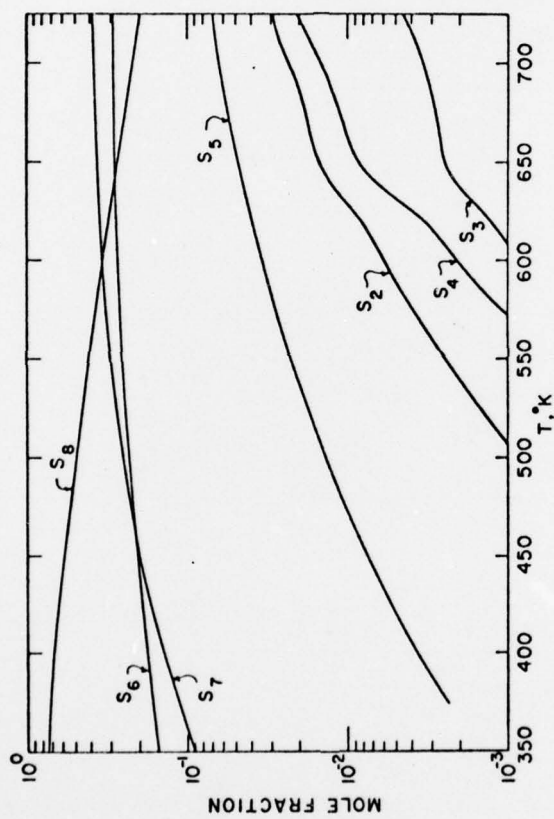


Fig 1. Concentrations of Various Sulfur Species in Saturated Vapor from Room Temperature to the Boiling Point of Sulfur.

polymers to form  $S_2$  molecules should occur very readily. Even though the species constituents of the gas change as a function of temperature, the total vapor pressure can be obtained as a function of temperature.<sup>31</sup> This functional relationship is shown in Fig 1a. Once the  $S_2$  molecules are formed, the behavior of the atomic, molecular and discharge electron processes become very important. This is discussed in the next section.

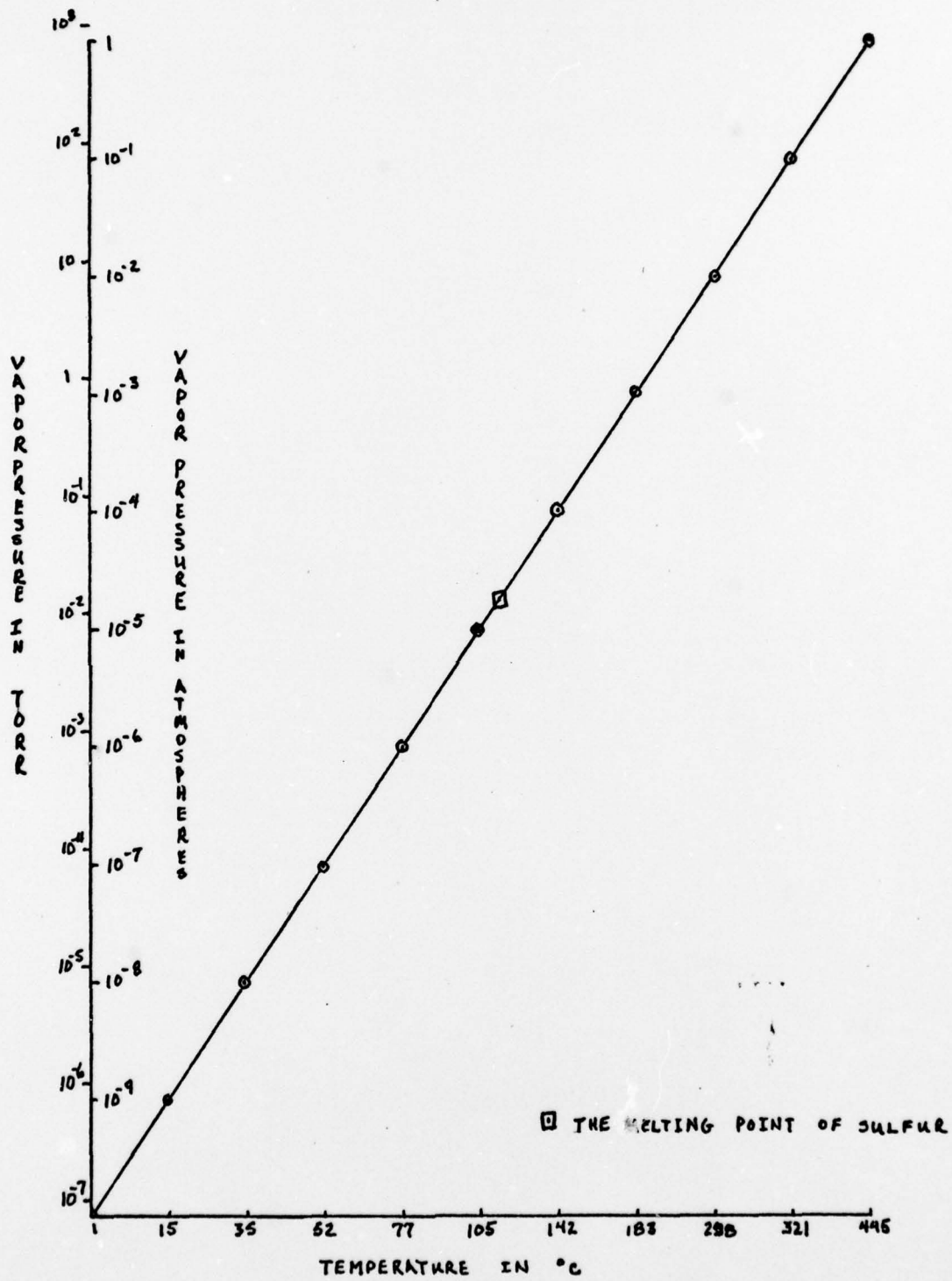


Fig 1a. Total Vapor Pressure of Sulfur vs Temperature.



## B. Electronic Structure, Discharge Physics, and Molecular Processes

In Figs 2-3 the atomic energy levels of S-atoms, along with the associated transitions, are presented.<sup>22</sup> From these figures it is immediately obvious that there exist five low lying energy levels at energies less than 3 eV. All of the transitions among these levels are forbidden with radiative lifetimes of approximately 1-sec, and consequently would be very difficult to observe<sup>20</sup>. The next highest levels are at 6 eV and would be expected only in a sulfur arc spectrum. In Fig 4, the approximate potential energy curves (PEC) of  $S_2$  are shown.<sup>1,22</sup> In the  $S_2$  system, the ground state  $X^3\Sigma_u^-$  is formed from two ground state atoms. The  $B''^3\Pi_u^-$  is also formed from two ground state atoms but is an excited state. The  $1u$  state is an unbound state and represents two ground state atoms coming together with no bond forming. Finally, the  $B^3\Sigma_u^-$  state is made up of one excited atom and one ground state atom forming an excited molecule. The levels  $v' \leq 9$  of the  $B^3\Sigma_u^-$  state are bound and strongly perturbed<sup>23</sup>. The levels  $v' \geq 10$  are not observed in emission, probably due to strong predissociation by the  $1u$  state of  $S_2$ .<sup>24</sup> The PEC of the two curves are fortunately displaced in their relative internuclear position so that the lowest vibrational levels of the  $B^3\Sigma_u^-$  excited state lie above high vibrational levels of the ground  $X^3\Sigma_g^-$  state which are not populated at temperatures as high as 600°C. The Franck-Condon factors for the B-X transition are as large as 0.1 for many bands and cover broad spectral ranges before diminishing.<sup>25</sup> The measured fluorescence lifetime of the individual states is approximately 45 ns.<sup>26</sup> The bands associated with this system extend from 2800 to 7000 Å. Emission from the  $B''^3\Pi_u^-$  state to ground has never been observed and

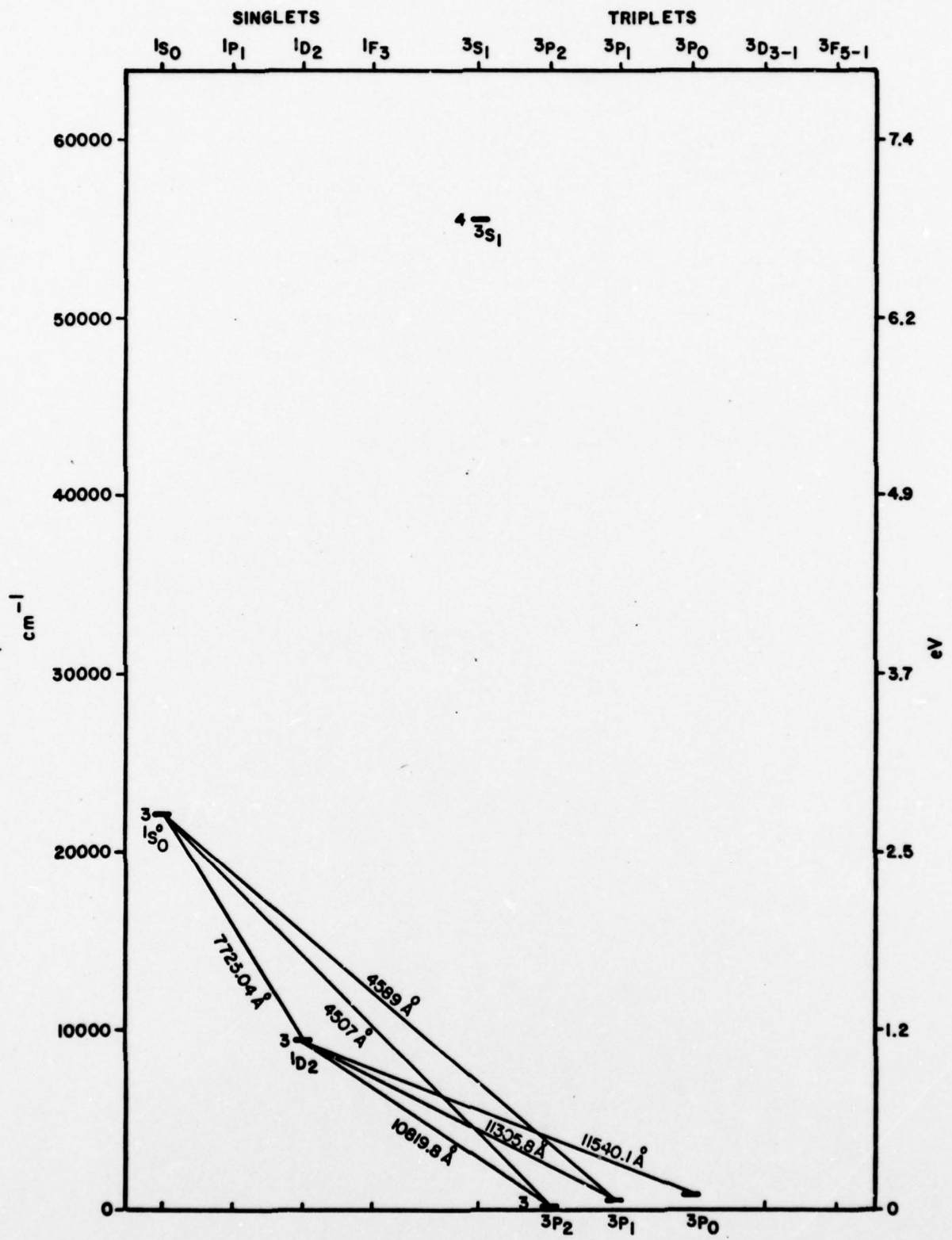


Fig 2. Low Lying Energy Levels of Atomic Sulfur.

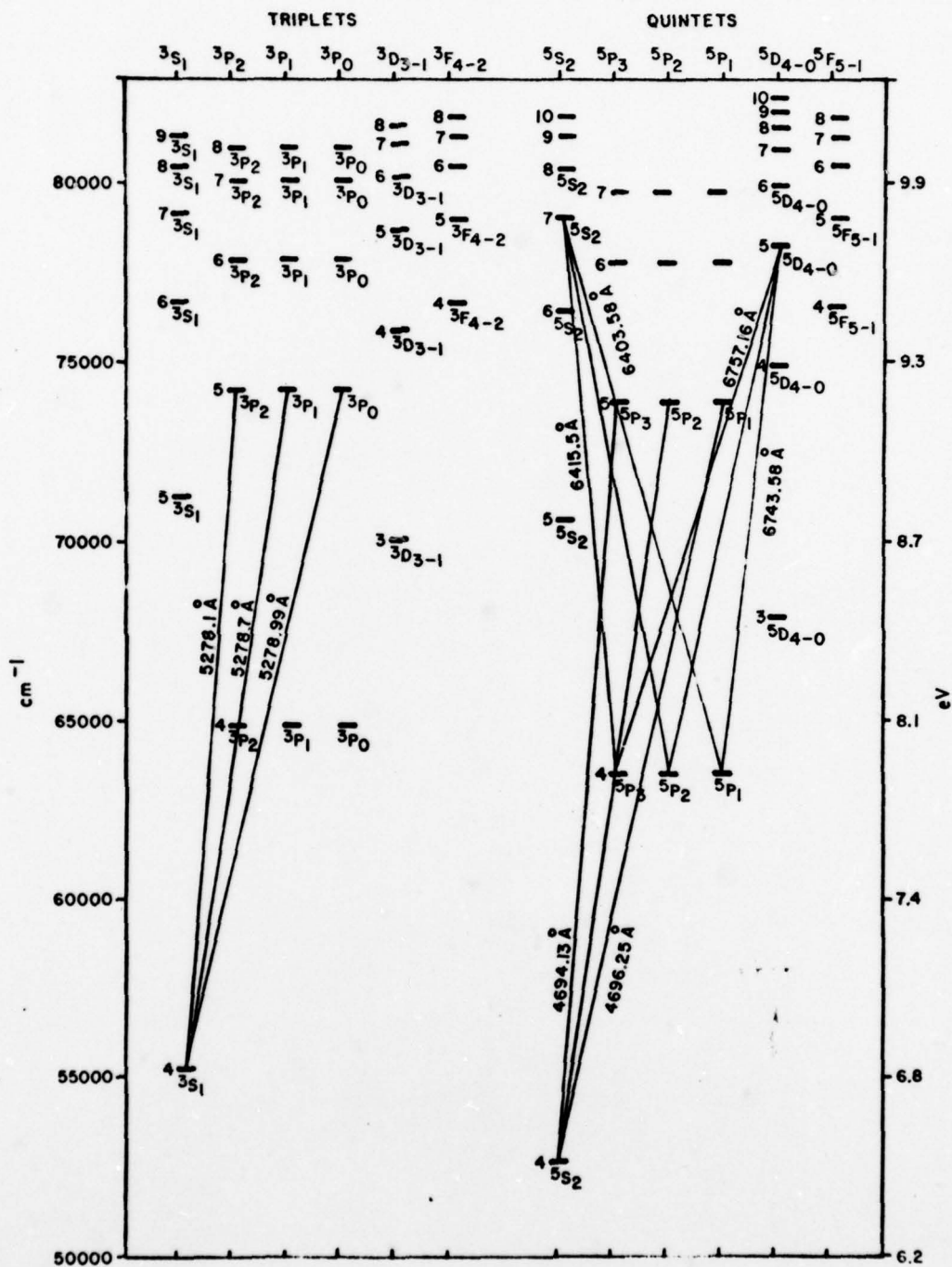


Fig 3. Higher Lying Energy Levels of Atomic Sulfur.

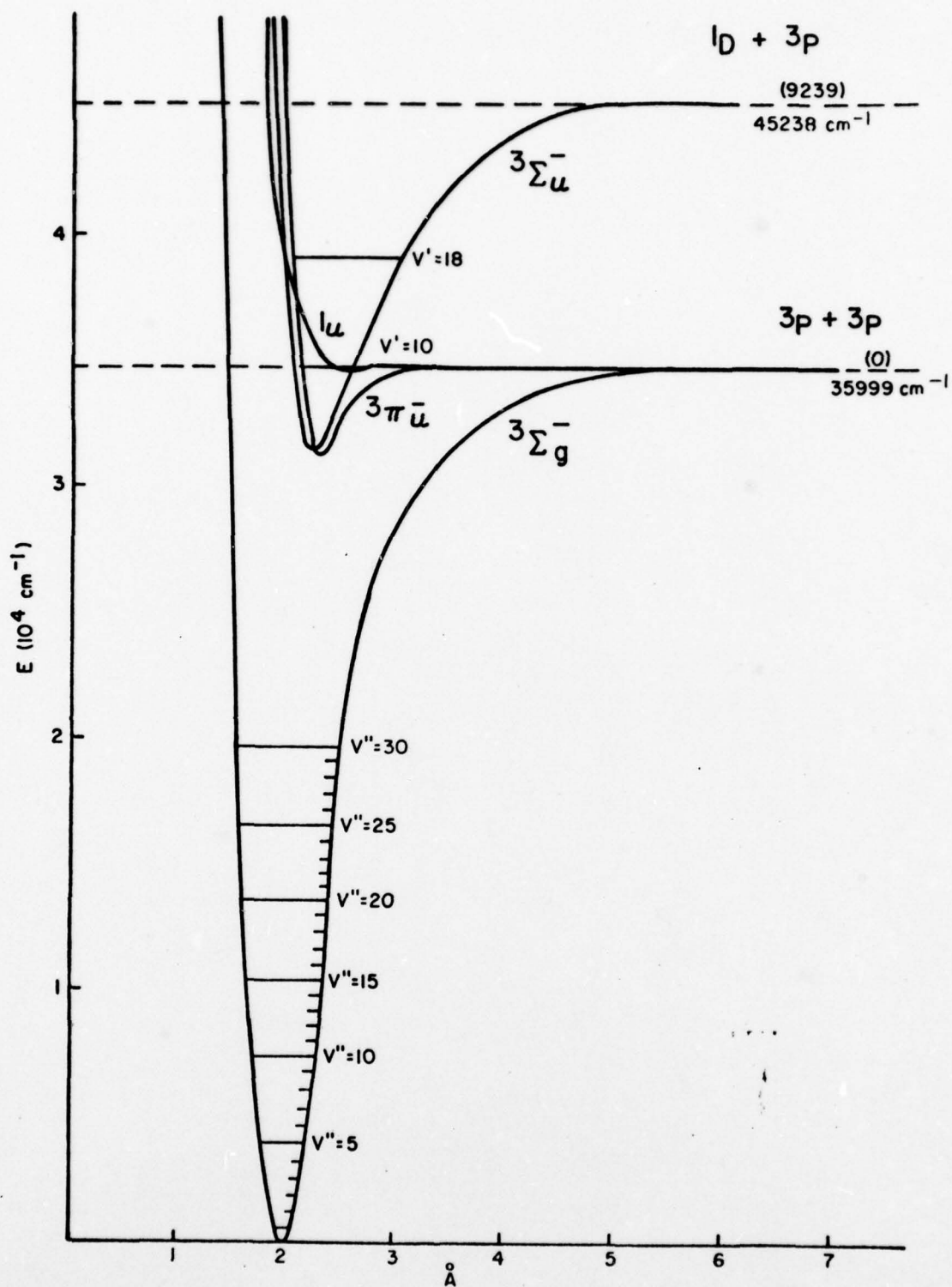
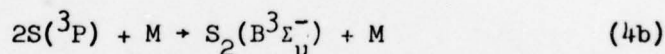
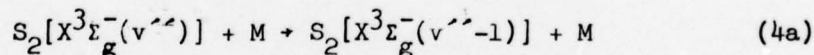
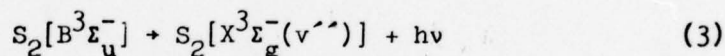
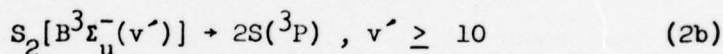
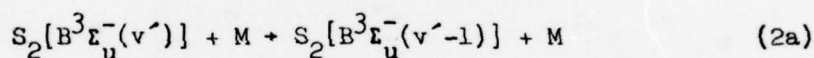
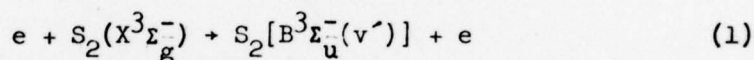


Fig 4. Some of the Approximate Potential Energy Curves of the  $S_2$  Molecule.

consequently negligible information on its characteristics is known. In Section IV data indicating the first observation of this transition is presented. The very unique feature of the  $S_2$  system is that all of the vibrational levels  $v' \leq 9$  of the  $B^3\Sigma_u^-$  state are below the dissociation energy of the  $X^3\Sigma_g^-$  ground state. Such a condition implies that negligible dissociation of the ground state should occur and hence eliminates the requirement for high pressure operation necessary for molecular formation.

The spectral discussed in Section IV could be interpreted using the following kinetic processes (no attempt is made here to completely describe the discharge).



where M is either an inert gas atom or  $S_2$  molecule. In step 1, electrons excite the ground state molecules to the excited  $B^3\Sigma_u^-$  state. Since the  $B^3\Sigma_u^-$  state is predissociated at  $v' = 10$ , the molecular processes diverge after Step 1. Above  $v' = 9$  the molecules would proceed via Step 2(b) where they are predissociated, to Step 4(b) where the separate atoms combine to give the  $B^3\Sigma_g^-$  state and the process can be repeated again. The other molecular process proceeds via Step 2, where the  $B^3\Sigma_u^-$  states are vibrationally relaxed. Subsequently, in

Step 3, they radiate via spontaneous and/or stimulated emission to a high vibrational level of the ground state which is then vibrationally relaxed in Step 4(a) and the cycle recurs with negligible dissociation of the  $S_2 (X^3\Sigma_g^-)$  state for this set of kinetic processes. The magnitude of all these processes except Step 3 are not known but it would be strongly expected that the electron impact cross section would be quite large. The reasoning for this is that optical transition between these two states is highly allowed and the largest cross sections are obtained for optically allowed transitions.<sup>27</sup> If such cross sections do exist, the electron energy distribution function should be strongly depleted for energies greater than 4 eV, the approximate threshold energy for the excitation of  $S_2$  from the ground to the excited state. In addition, very high electron power transfer into the  $B^3\Sigma_u^-$  state should occur. The exact details of this effect have not been pursued in this thesis because of time constraints.

### III. EXPERIMENTAL TECHNIQUES

In Fig 5, a schematic of the experimental arrangements is shown, and in Fig 6, a photograph of the actual experiment is exhibited. The identical set-up was used for both the CW and pulsed experiments, only the excitation source was changed. The discharge tubes were placed inside of a pyrex (Borosilicate glass - Corning Glass Works 7740) tube that had a heater/blower attached to one end. This arrangement provided uniform heating of the tube to within  $\pm 3^{\circ}\text{C}$ . Even for CW experiments where large gas heating occurred, such temperature uniformities were acquired. Attempts to run the tube in a Sola Basic Lindberg furnace at  $200^{\circ}\text{C}$  resulted in an overpressure extinction of the discharge after only a few seconds of discharge operation. With the shield however, running the discharge was accomplished by using the heater to raise the temperature. Then, after obtaining breakdown, as the discharge ran the external heat was removed or decreased until the desired operating temperature was attained. After equilibrium was achieved, the type of discharge was varied by adjusting the temperature. A quartz observation window was used in order to examine spectra down to  $2500 \text{ \AA}$ . The discharge tube was mounted vertically in order to allow maximum light to enter the spectrograph. This discharge light was collected by a 5 cm diameter, 25 cm focal length lens and focused on the entrance slits of a Model 216.5 meter GSA/McPherson scanning spectrometer/monochromator (f/8.7), having a 1200 g/mm grating blazed at  $5000 \text{ \AA}$ . For wavelengths above  $5600 \text{ \AA}$ , a lower cutoff filter was used to eliminate the second order spectra. The lens and viewing window were scanned with a Varian Cary 219 spectrophotometer to insure their transmissivity down to  $2500 \text{ \AA}$ . Then a scan of a calibrated tungsten halogen lamp (#EPI-1595) operated at 7.9 amperes was made.

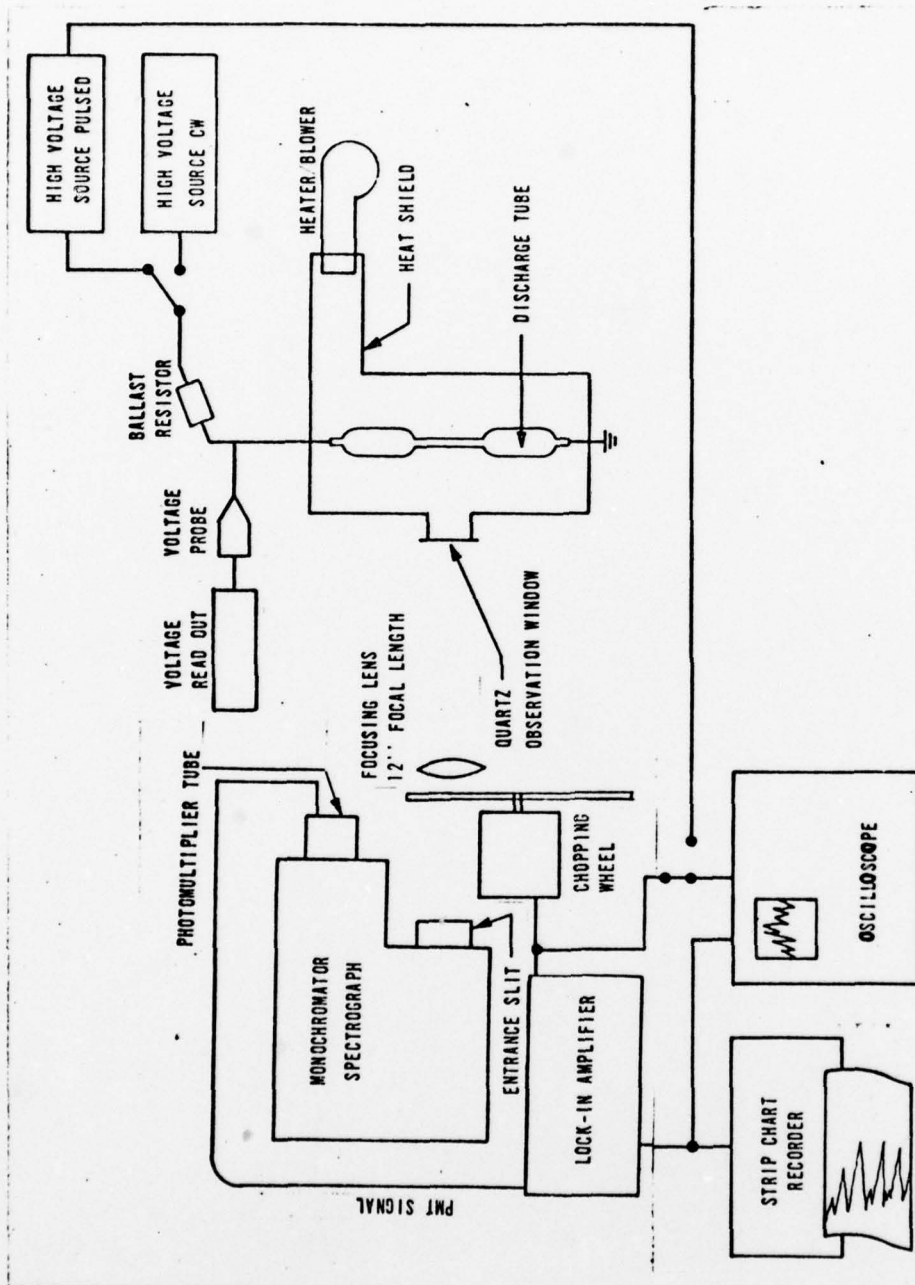


Fig 5. The Experimental Setup - Pictured Schematically.



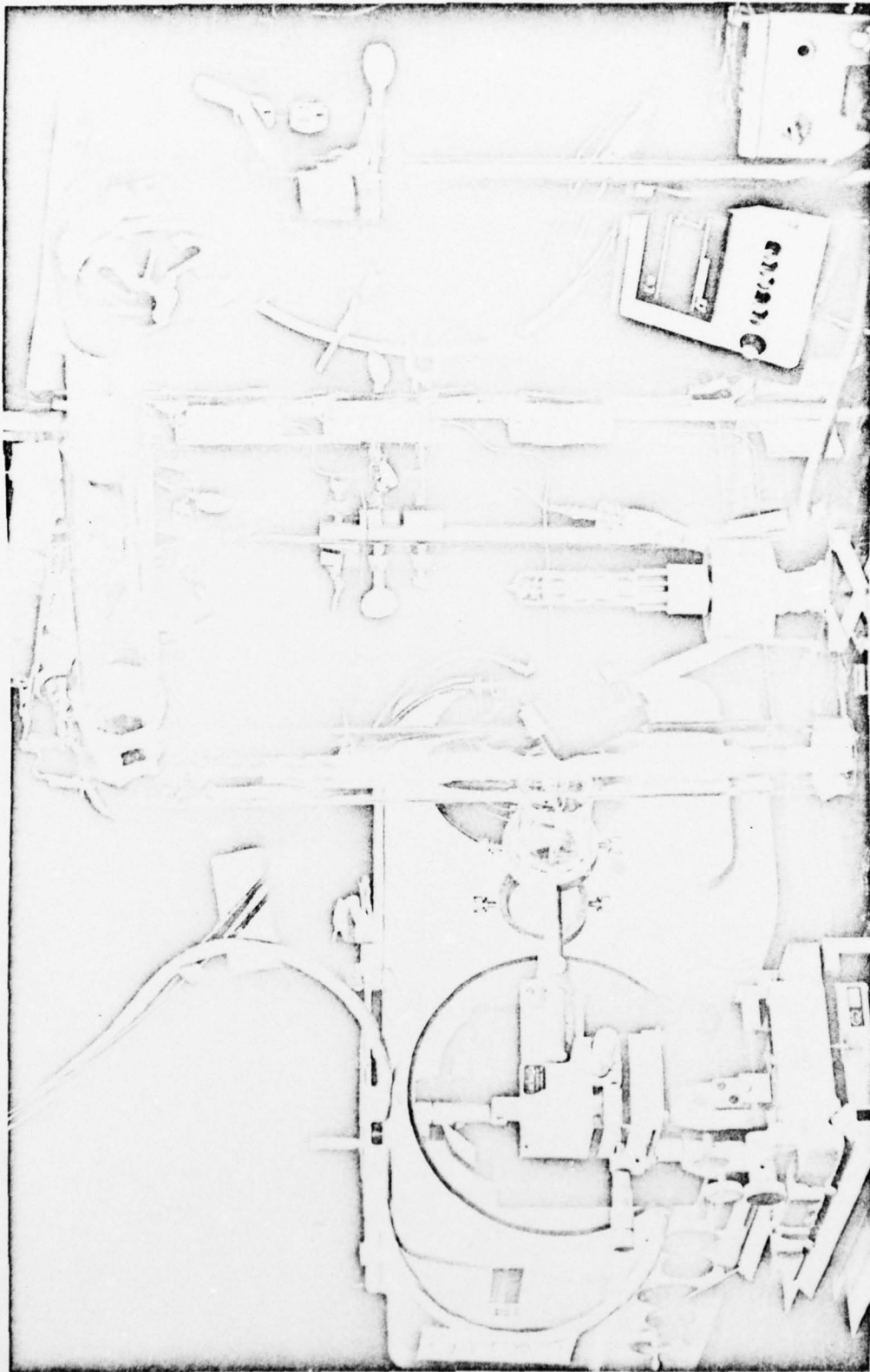


FIG 6. Actual Experimental Setup.

The system was linear from 2500 Å to 7000 Å. The photomultiplier (PMT) was an RCA 31034A. Most data was taken with a slit width of 10 microns, which gave a final first order spectral resolution of .4 Å. For time-integrated spectrographs, the exit slits were replaced by a Polaroid Land Back Film Holder.

For accurate scanning of the observed spectra, a Princeton Applied Research (PAR) Model 192 variable frequency light chopping wheel was placed between the lens and the entrance slit. It was positioned such that all the light from the lens was chopped. The output from the PMT was connected in parallel to a PAR Model 124 lock-in amplifier and an oscilloscope, as was the reference chopping frequency of 200 Hz. The oscilloscope was used to monitor the real-time spectra as it was being scanned. The chopping frequency was carefully controlled and the lock-in amplifier was tuned for optimum frequency and phase match conditions. The output of the lock-in amplifier was recorded on a Hewlett-Packard 7100B strip chart recorder, Model 17500A. The monochromator scan speed (and the time constant on the lock-in amplifier) were selected such that the observed spectra were insensitive to the scan speed. Time integrated spectra were taken in both the pulsed and CW modes, while strip chart spectra were taken only in the CW mode. Electrical noise during pulsed operation eliminated strip chart spectra recording.

The voltage drop directly across the tube was monitored by a Tektronix Model P6015 high voltage probe and read on a Model 3439 H-P digital voltmeter (DVM) for CW operation and recorded on an oscilloscope for pulsed operation. For CW excitation the D.C. current was measured via the high-voltage power supply and for pulsed operation a Model 110 Pearson transformer was used. In CW operation, a current regulator (< 1% fluctuation) and a series resistor were used. For pulsed conditions,

only a series resistor was used to control the current. The sulfur discharges were stable enough that no current regulation was required. The D.C. high voltage was supplied by a Kilovolt high voltage power supply and then pulsed by a Tachisto pulser. A series resistance was necessary to offset the effects of the negative resistance of the discharge tube, and to keep the current from running away at breakdown. Resistances of  $50K\Omega$  were generally used, because analysis of the voltage-current (VI) characteristics of the tube indicated an approximate resistance of  $38K\Omega$  (negative) at breakdown.

The tubes used in the discharge studies were constructed of quartz (vitrious silica - Amersil T08), tungsten feed-throughs, and Hastelloy (C-276) electrodes (see Appendix A). The tungsten fees, with G.E. glass to metal seals and graded seals to quartz, were obtained from new ILS Xenon flashlamps which were dissected, only the feed-throughs being used. Hastelloy pellets in the form of a small cylinder .95 cm in diameter and .95 cm in length were manufactured and used as the electrodes. They were attached to the tungsten feeds by a set screw, and positioned such that a minimum of the feed was exposed to the sulfur. Hastelloy was selected because it showed good resistance to attack by the  $S_2$  vapor (see Appendices B and C). Although Al and Mg are even more resistant, they would not stand up to the temperatures needed in construction of the tube. Just prior to assembly the electrodes were sandblasted. After attaching the electrodes to the prepared feeds, a quartz envelop was fashioned around the electrodes, leaving approximately .3 cm clearance to the inside of the tube, and approximately 25 cm separation between the electrodes. Centered between the electrodes the main area of the discharge tube was necked down to a diameter of .9 cm over a length of 12.5 cm. When the tube was fully assembled, the pump-out port

was attached and the tube cleaned with methyl alcohol and acetone. Then the tube was baked at about  $500^{\circ}\text{C}$  for four hours under a constant vacuum of  $10^{-6}$  torr.

The sulfur was prepared from 99.9999% ultra pure granular stock obtained from Research Organic/Inorganic Chemical Corp. The ultra pure sulfur was placed in a small ampule, which was then evacuated. The ampule was evacuated using a tube which went through a cold trap. As the ampule was heated, any adsorbed gases in the sulfur or any other impurities lighter than sulfur would be driven off and collected in the trap (see Appendix C). After heating and while still under vacuum, the ampule was sealed off. The ampule of sulfur was then placed in a specially prepared section of the evacuation port. The entire apparatus was evacuated to  $10^{-6}$  torr, and isolated from the vacuum source. Helium could then be introduced into the tube at a fixed pressure and finally the tube and port were sealed off. The He kept the cathode cooler, allowing for longer tube life. The ampule was constructed with a small hook on one end so that a slight impact would break the ampule. After the tube and port were sealed off, the ampule was broken and the sulfur driven into the tube by heating the port/ampule, and finally the port was sealed off and removed from the tube. Any contaminants heavier than the sulfur would be left in the ampule. During the discharge the electrodes were attacked by the  $\text{S}_2$  vapor. The cathode attack was especially severe, resulting in flaking off of the cathode surface and in deposits of the Hastelloy constituent metals appearing on the inside surface of the quartz envelope (see Appendix C). After a few hours of operation, the entire cathode area was so discolored from the deposits that the electrode was no longer visible. The cathode was more severely attacked because of its elevated temperature; the sulfidation process being

enhanced by higher temperatures. The cathode heating was caused by the heavy  $S_2$  ions accelerating through the cathode fall region and striking the electrode surface. Because the sulfur attacks the electrodes, an amount in excess of that needed to give 50 torr vapor pressure (VP) at  $300^\circ C$  was used. The extra sulfur allowed some to be chemically removed by combining with the metals of the Hastelloy, yet have the discharge continue. In most cases about 1 gram of sulfur was sufficient. The VP of the metal sulfides formed was so low that they did not interfere with the discharge.<sup>31</sup>

#### IV. RESULTS AND ANALYSIS

##### A. Discharge Characteristics

The  $S_2$  discharge is white in color with a slight bluish tinge. The discharge is amazingly stable, unlike those of  $O_2$  which are unstable.<sup>33</sup> At low pressures the discharge demonstrates all the typical characteristics of low pressure glow discharges. The cathode dark space and negative glow are quite distinct, as is the anode glow. As the discharge is operated at higher currents/temperatures, the emission from the positive column that forms is bright enough to light the room. During pulsed operation, there is a very definite change in the appearance of the discharge as the internal temperature goes through  $159^{\circ}C$  and the sulfur rings thermally break up; the emission changes from pale bluish white to a bright almost white discharge.

The voltage-current (VI) characteristics of the discharge were very difficult to obtain because the discharge is so sensitive to temperature. If the applied voltage is changed slightly, the temperature changes almost at the same time. So much of the heat necessary to run the discharge is coming from the discharge, that changing the discharge will very rapidly change the temperature. To take the VI measurements shown in Fig 7, an imprecise but adequate method was developed. The tube was allowed to stabilize at a particular current setting. The voltage was rapidly changed and the new current reading recorded. Then the voltage was reset and the tube allowed to stabilize again. After stabilization the voltage was varied to a different setting and a current reading taken. This process was repeated until the voltage/current readings were recorded down to extinction/breakdown of the discharge.

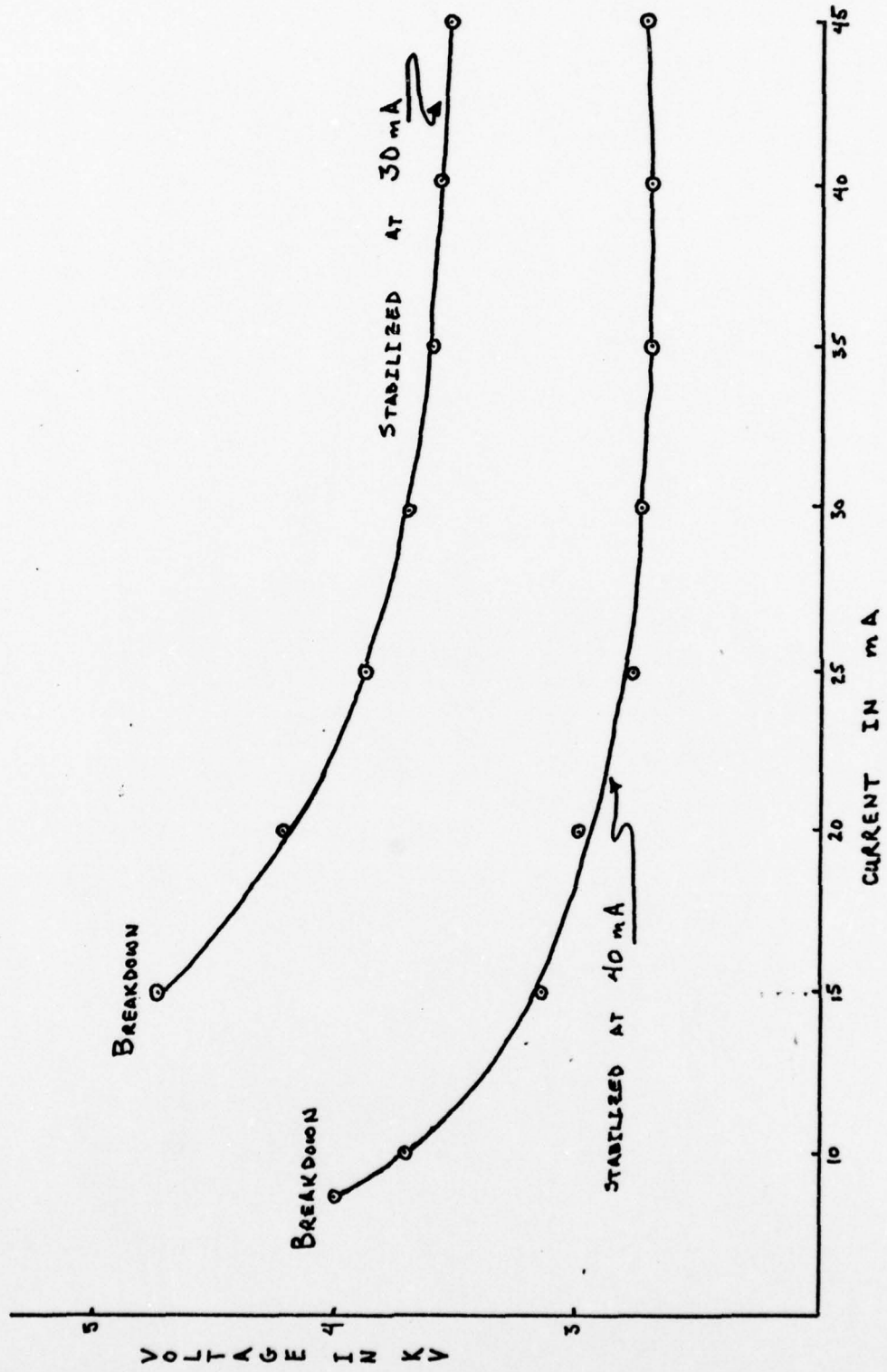


Fig 7. VI Characteristics of a Sulfur Discharge Tube.

As the VI curve shows, the  $S_2$  discharge is a negative impedance discharge and over the range of operating parameters used, responds like a negative resistance. The  $S_2$  discharge is a very stable, self-sustaining discharge with almost no fluctuations in voltage or current. As the temperature/current is increased, the positive column does constrict, but within the limits of the equipment used, the discharge never goes into an arc. Because of the well-behaved nature of the discharge, excessive attachment does not appear to be a problem in sulfur discharges. Typical power loading on the tube was 2.82 watts/cc with a maximum of 3.5 watts/cc cw operation, where the high voltage power supply was the limiting factor. Much higher power loadings could be achieved during pulsed operation. (12.8 watts/cc were achieved).

Once the problems with tube construction and sulfur purification had been solved, and the sulfur discharge could be maintained indefinitely at any desired power loading/current, then attention could be given to the analysis of the spectral character of the discharge. This is presented in the next section.

#### B. Spectra

Spectra were obtained, using the experimental set-up described in Section II. When taking the spectra, a He-Ne laser and a Hg lamp were used as reference sources. The reference lines were recorded simultaneously with the  $S_2$  discharge, so the reference lines are superimposed directly on the  $S_2$  spectra. The many Hg lines allow accurate wavelength determination periodically in the spectra and thus serve as a cross check to the linearity of the entire system.

Since the emitted light appears bluish white, the spectra should cover the whole visible spectrum, but perhaps have greater intensity in



the blue. A typical spectra of  $S_2$  is shown in Fig 8, and as expected, there is band emission evident from the UV through the visible, with a noticeable increase in intensity toward the UV. The band system cuts off sharply at  $2800 \text{ \AA}$  and stops less noticeably at about  $6200 \text{ \AA}$ . The bands themselves are degraded to the red and form a regularly spaced progression between  $6200 \text{ \AA}$  and  $5000 \text{ \AA}$ . Below approximately  $5000 \text{ \AA}$  the regularity ceases, although the system is still obviously band structure (molecular) and not atomic line structure. The few atomic lines which are seen are those of impurities, mostly from the Hastelloy; no sulfur atomic lines are evident. In Fig 8, the band at  $5660 \text{ \AA}$  is actually a second order of the  $2828.9 \text{ \AA}$  band; the rest of the second order bands were removed using a band pass filter.

Time integrated spectra of CW and pulsed discharges were taken to determine if there were differences in the observed spectra, and some typical examples are shown in Fig 9. The same characteristic sulfur spectrum was obtained in both cases. The spectra of the He-sulfur tube also gave the sulfur spectrum. Adding the He only aided in heat distribution, and cooling the cathode. The He-sulfur tube did glow orange with He emission at low temperatures (which made the  $S_2$  VP about  $10^{-5}$  torr), but that glow disappeared as the temperature increased and the  $S_2$  discharge appeared.

Strip chart spectra were taken with the tubes in many different power loading configurations, and with discharges that ranged from low pressure stable discharges to high pressure constricted discharges. All the spectra appeared identical; displaying only the  $S_2$  spectrum. Thus the  $S_2$  system appears to behave the same under low and high power operation.

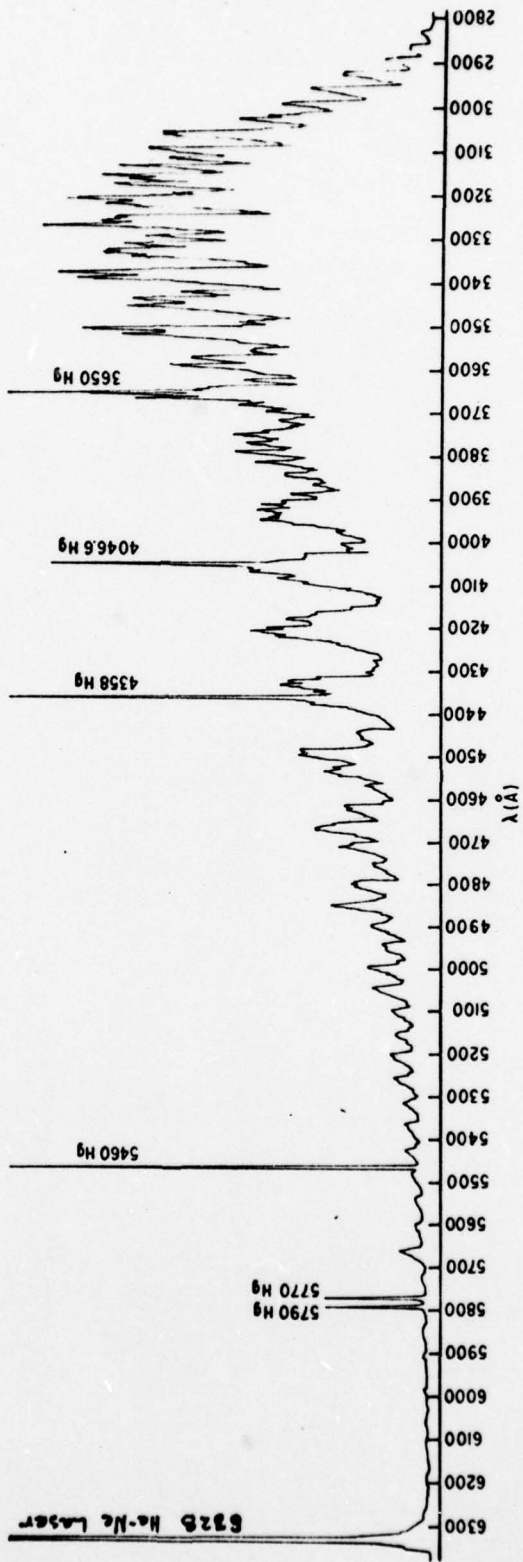


Fig 8. A Strip Chart Emission Spectra of the S<sub>2</sub> Molecule.

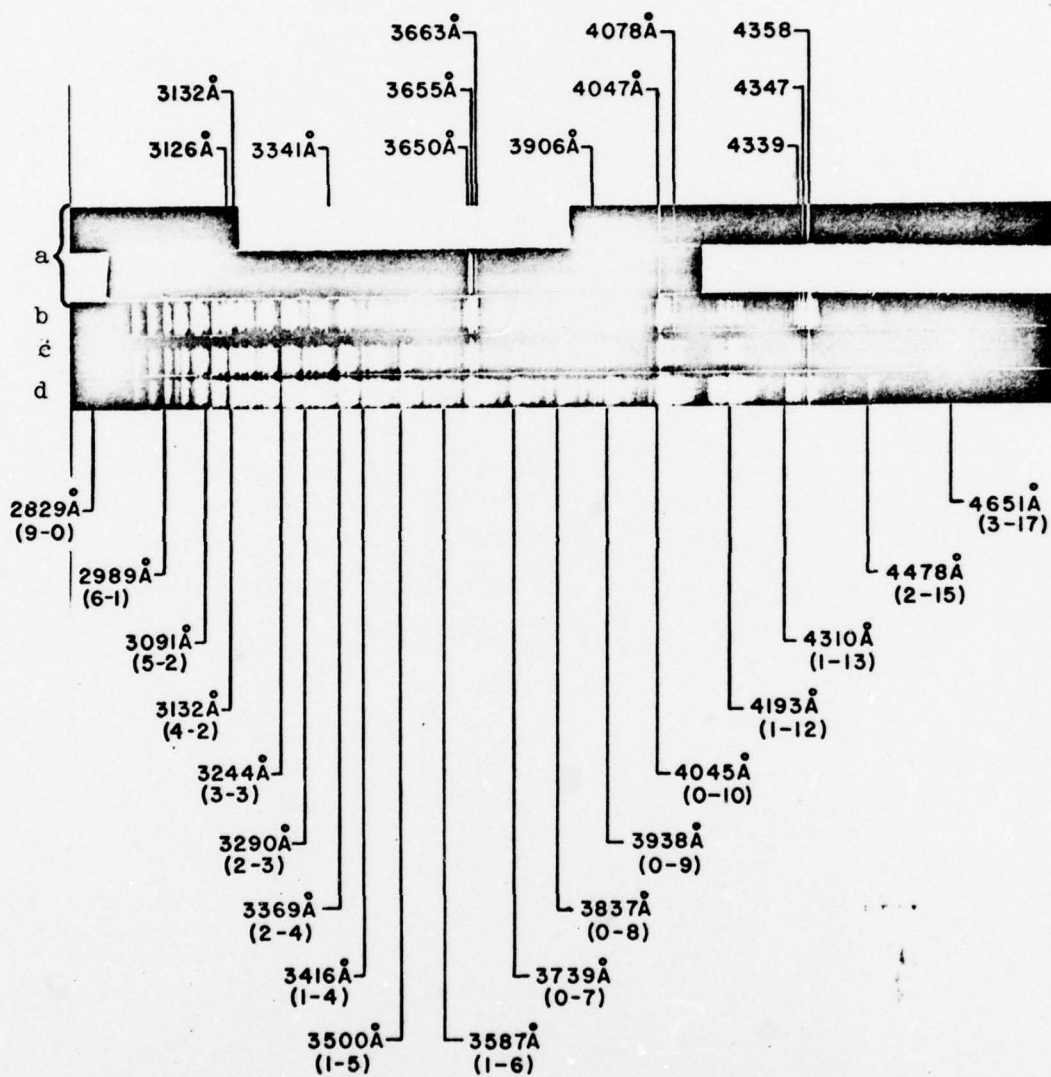


Fig 9. Time Integrated Emission Spectra of the S<sub>2</sub> Molecule.  
 a) The Hg reference lines, b) CW Emission, c) pulsed emission (4.2 watts/cc), d) pulsed emission (12.6 watts/cc).

Analysis of the spectrum was started by taking the previously observed transition and energy level designations<sup>28,29</sup> of the  $B^3\Sigma_u^- - X^3\Sigma_u^-$  system and identifying each one on the spectra. They were all present and easily identified. There was, however, considerable structure that was not identified. It was decided to calculate the entire array of wavelengths which should be in the  $B^3\Sigma_u^- - X^3\Sigma_g^-$  system and see how many could be identified. For emission, the  $S_2$  (B-X) system only contains transitions from  $v' \leq 9$  because the  $B^3\Sigma_u^-$  state is predissociated at  $v' = 10$  by the  $1u$  state. This is why the band system is so markedly cut off at 2828.9 Å and 6166 Å. There would be transitions possible from  $v' \leq 9$  at wavelengths higher than 6166 Å, but the Franck-Condon factors are so small for those transitions that they were not observed.

The spacing between vibrational levels can be expressed as a general expansion in  $(v'' + \frac{1}{2})$  as follows:<sup>32</sup>

$$(1) \bar{\nu} = \bar{\omega}_e''(v'' + \frac{1}{2}) - \bar{\omega}_e X_e''(v'' + \frac{1}{2})^2 + \bar{\omega}_e Y_e''(v'' + \frac{1}{2})^3 - \bar{\omega}_e Z_e''(v'' + \frac{1}{2})^4 + \dots$$

where  $\bar{\nu}$  is the wavelength of the transition in  $\text{cm}^{-1}$ , and  $v''$  is the vibration level number in the ground state.  $\bar{\omega}_e$  is the oscillation frequency in  $\text{cm}^{-1}$ , and  $\bar{\omega}_e X_e$ ,  $\bar{\omega}_e Y_e$ ,  $\bar{\omega}_e Z_e$  ... are higher order correction factors called anharmonicity constants. The more the potential energy curve deviates from that of a simple harmonic oscillator (SHO), the higher the order of anharmonicity constant needed to adequately describe the curve.

Using the known transitions and (1) it was determined that anharmonicity constants up to the quartic or  $\bar{\omega}_e Z_e$  were necessary to obtain agreement up to  $v'' = 30$ . The values obtained were 1)  $\bar{\omega}_e = 727.85 \text{ cm}^{-1}$ ,

2)  $\bar{\omega}_e X_e = 3.019 \text{ cm}^{-1}$ , 3)  $\bar{\omega}_e \psi_e = .0042 \text{ cm}^{-1}$ , and 4)  $\bar{\omega}_e Z_e = .0000098 \text{ cm}^{-1}$ .

The spectroscopic constants were acquired by solving five simultaneous equations relating the observed wavelengths to eqn. (1). Very similar values were obtained from each level of the  $B^3\Sigma_u^-$  state, calculated independently, implying that the constants are good and also that the designations of the transitions as they are now, is correct. A similar computation for the upper state is not possible, because it is perturbed.<sup>23-30</sup>

Using these values for the ground state constants, the wavelengths for each upper level of the  $B^3\Sigma_u^-(v')$  to all the  $X^3\Sigma_g^-$  levels ( $v''$ ) up to  $v'' = 35$  were calculated. These calculated values were then compared with all the known wavelengths. Complete agreement to within  $1.5 \text{ \AA}$  on almost every transition was obtained. Most calculated wavelengths were within  $.5 \text{ \AA}$ ; it was only at the higher ground state vibrational levels ( $v'' > 30$ ) that precise agreement started to deviate. Apparently the potential energy curve for the  $X^3\Sigma_g^-$  state is one which departs rather drastically from the simple harmonic oscillator model. To obtain a good fit above  $v'' = 30$  even higher order anharmonicity constants than quartic would have to be used.

As further evidence about the nature of the ground state potential energy curve, the  $v''$  maximum term was calculated. Since the  $v''$  states converge (get closer together as  $v''$  increases), they eventually reach a limit which would correspond to the dissociation limit of the molecule. Using the above constants,  $v''$  maximum would be 119. The dissociation limit associated with  $v'' = 119$  would be  $49,975 \text{ cm}^{-1}$ . The predissociation limit of the  $B^3\Sigma_u^-$  determined by Ricks and Barrow<sup>24</sup> using analysis of the rotational structure is  $36,000 \text{ cm}^{-1}$ . Because the lu dissociating state originates from the  $^3p + ^3p$  combination, as does the  $X^3\Sigma_g^-$  state, where the lu state predissociates the  $B^3\Sigma_u^-$

state would be at least as great as the dissociation limit of the ground state. Since the  $1u$  state is shallow when it intersects and predissociates the  $B^3\Sigma_u^-$  state at  $v'' = 10$  this predissociation limit of  $36,000\text{ cm}^{-1}$  can be taken as a good approximation of the dissociation limit of the ground state. The predicted limit of  $49,975\text{ cm}^{-1}$  from  $v''_{\text{max}} = 119$  is grossly in error. A  $v''$  of 66 would correspond to approximately  $36,000\text{ cm}^{-1}$ . This is yet another indication that the  $B^3\Sigma_g^-$  state potential curve is departing drastically at higher values of  $v''$  from the SHO model.

As already mentioned, however, the quartic term gives excellent agreement, at least through  $v'' = 30$ . This entire array of calculated wavelengths, covering all the transitions in the  $B^3\Sigma_u^- - X^3\Sigma_g^-$  system from  $v' = 9$  to 0 and  $v'' = 21$  to 0 was diligently compared with the spectra from the  $S_2$  discharges. Tables 1 and 2 given a Deslandres table representation of these comparisons. The upper wavelengths are the known/calculated values and the lower wavelengths are the experimentally observed ones. As can readily be seen, the agreement is excellent. Not only are the dominant transitions that have been observed previously, easily observed, but virtually every transition is observable.

Using selective excitation, Meyer and Grosley<sup>25</sup> have determined the Franck-Condon factors for  $v' = 3$  and  $v' = 4$  of the  $S_3$  (B-X) system. The experimentally observed intensities correspond exactly to the intensities/Franck-Condon factors they reported. This is still further verification that the  $S_2$  (B-X) system is correctly identified.

The Deslandres table was continued up to  $v'' = 35$  where the departure in calculated wavelengths was as much as  $13\text{ \AA}$ . This departure, however, increased rapidly after  $v'' = 30$  where it was only about  $1.5\text{ \AA}$ . Agreement between the calculated and observed data was still excellent. The spectra taken in this region was not as detailed, however, so the

Table 1. The Deslandres Table of the  $B^3\Sigma_u^- - X^3\Sigma_g^-$  System ( $v'' \leq 10$ ).

$v'$	0	1	2	3	4	5	6	7	8	9	10
0	3156.7	3230.3	3306.8	3387.0	3469.6	3555.8	3645.2	3740.0	3837.3	3939.1	4045.8
			3307	3387.0	3469.6	3555.8	3645.2	3740	3837.3	3938.9	4045.8
1	3113.1	3184.7	3259.9	3336.7	3417.0	3500.5	3587.4	3677.3	3771.5	3870.0	3973
		3185	3259.9	3336.5	3417	3500.5	3587.4	3677.3	3771.1	3871	3973.7
2	3073.7	3143.7	3216.1	3290.7	3369.8	3451.0	3534.5	3622	3713	3811	3909.6
		3143.7	3216.1	3290.7	3369.6	3451	3534.3	3621.9	3713.9	3810.8	
3	3033.1	3105.5	3175.5	3244.7	3321.2	3399.0	3480.9	3566.1	3654.7	3747.1	3843.4
	3033.1	3105.5	3175.5	3244.7	3321.2	3399.1	3481.5	3567.4	3654.9	3749	
4	2997.0	3063.6	3132.4	3203.2	3277.0	3353.8	3433.4	3516.3	3602.5	3692.2	3785.6
	2997.0	3063.6	3132.4	3203.2	3275.9	3354	3434.2	3516.7	3602	3692.5	3787.3
5	2960.1	3024.8	3091.7	3161.1	3233.0	3307.6	3385.1	3465.6	3549.3	3636.3	3727.0
	2960.1	3024.8	3091.7	3161.1	3232.7	3308		3466	3550	3636.2	3727.3
6	2926.6	2989.7	3054.9	3122.9	3193.1	3265.8	3341.4	3419.8	3501.2	3585.9	3674.0
	2926.6	2989.7	3054.9	3119.5	3192.6	3266	3340.6	3419.8	3501.7		3672.6
7	2892.5	2954.2	3018.0	3084.1	3152.5	3223.4	3297.0	3373.3	3452.5	3534.8	3620.4
	2892.5	2954.2	3018	3084	3152.9			3373.7	3452		3620.4
8	2860.1	2920.4	2982.7	3047.3	3114.1	3183.2	3255.0	3329.3	3406.5	3486.6	3569.8
	2860.1	2910.4	2983	3046.5	3114.2	3183	3254.9	3329.3	3406.6	3487	3570
9	2828.9	2888.1	2948.8	3011.9	3077.1	3144.6	3214.6	3287.1	3362.3	3440.3	3521.3
	2828.9	2888.1	2948.8	3012	3078	3144	3214.8	3286	3362	3438.8	3520.5

Table 2. The Deslandres Table of the  $B^3\Sigma_u^- - X^3\Sigma_g^-$  System ( $v'' > 10$ ).

$v'$	11	12	13	14	15	16	17	18	19	20	21
0	4157.2 4157.2	4274.4 4274.4	4395.0 4395	4523.5 4523.5	4657.6 4657.3	4799.4	4948.7	5106.1	5272.3	5448.0	5634.1
1	4081.0 4081	4193.8 4193.8	4311.0 4311	4433.6 4433.6	4563.2 4563.2	4699.0 4699	4842.3	4992.9	5151.7	5319.4	5496.6
2	4012.8 4012.5	4121.5 4120.8	4235.2 4235.8	4355.0 4355	4478.8 4478.8	4610.0 4610	4747.6 4747.6	4893.8	5044.7	5205.4	5375.0
3	3943.9 3944.2	4048.8 4048	4158.5 4158.3	4273.2 4273.2	4393.4 4393.8	4519.3	4651.3 4651.3	4790.8 4790.8	4937.2	5090.9	5252.1
4	3883.1 3884	3984.8 3983.9	4090.9 4090.8	4201.9 4201.6	4318.1 4318	4439.6 4440	4567.1 4567	4700.9 4701	4842.2	4990.1	5145.5
5	3821.4 3820.3	3919.8 3920.2	4022.5 4021.6	4129.8 4130.3	4241.9 4242	4359.2 4359	4482.0 4482	4610.7 4610	4745.8	4887.7	5036.8
6	3765.7 3767	3861.3 3861.5	3960.9 3961	4064.8 4064.6	4173.4 4173.6	4286.9	4405.6 4406.5	4529.9	4660.3 4660	4797.1 4797	4940.7
7	3709.4 3709.2	3802.1	3898.7 3898.8	3999.4 4000.4	4104.4 4103.2	4214.1 4214.8	4328.8 4329	4448.8	4574.4 4574.7	4706.1 4705.8	4844.3
8	3656.3 3658	3746.3	3840.0	3937.7	4039.5 4039.2	4145.7 4145	4256.6 4257.6	4372.6 4373	4493.9 4494	4620.9 4621	4754.1
9	3605.5 3605.7	3693.0 3693	3784.0 3783	3878.8	3977.5 3977.9	4080.5 4080.3	4187.9	4300.1 4300	4417.3	4540.0 4540	4668.5 4668.3



less precisely determined values are not given here. But, as stated, the agreement is excellent all the way to  $6166.9 \overset{\circ}{\text{A}}$  where the band system stops because the upper limit is predissociated at  $v'' = 10$ .

Even after all the transitions of the  $S_2$  (B-X) system have been accounted for, there is still considerable structure that is left unexplained. The overall appearance of the spectra would tend to indicate that another system of bands is overlapping or superimposed on the  $S_2$  (B-X) system. Three possible explanations of this unexplained structure are 1) it could be arising from the different isotopes of sulfur existing in the tube at the same time - each isotope would have slightly different internuclear spacing and thus slightly different transitions; 2) the additional structure could arise from other polyatomic molecules of sulfur which may be in the tube. For example,  $S_4$ ,  $S_6$ , and  $S_8$ ; and finally 3) the structure could be from another molecular state of  $S_2$ . Of these three, the third is by far the most likely, because the concentrations of rarer isotopes of sulfur are generally quite small, and the band structure from polyatomic molecules would be expected to be much more complicated than the system we are left with after removing the  $S_2$  (B-X) transitions. It is thought that the  $B\overset{-}{\Sigma}_u$  state is perturbed by the  $B''\overset{-}{3}\pi_u$  state<sup>24</sup>, which would make the  $B''\overset{-}{3}\pi_u$  state a very eligible candidate as the origin of the unexplained structure. Until now, however, no one has reported seeing emission arising from transitions between the  $B''\overset{-}{3}\pi_u$ -X states.

The unexplained structure consists of many small (and a few large) transitions that run all along and on top of the larger structure from the (B-X) system. If the  $B''\overset{-}{3}\pi_u$  state is close enough to perturb the  $B\overset{-}{3}\Sigma_u$  state, then it should radiate to the ground state just as the  $B\overset{-}{3}\Sigma_u$  does. If that were the case, then the ground state spacing which

is already known from the (B-X) system should help to unravel the new system.

Working under the assumption that the  $B''^3\Pi_u^-$  state is radiating to the  $X^3\Sigma_g^-$  state, and already having the ground state spacing, the Deslandres table for the  $B''^3\Pi_u^- - X^3\Sigma_g^-$  system can be constructed. One method for doing this would be to pick one of the unidentified transitions, then assume it is a particular  $v''$  transition. Using the known ground level spacings which can be calculated using the oscillation frequency and anharmonicity constants derived earlier, the next higher  $v''$  and next lower  $v''$  can be predicted. These predictions are compared with the spectral data. If the predicted wavelengths are not found in the experimental data then assume the chosen wavelength is another  $v''$  and again predict the next upper and next lower transitions. Again compare the predicted values to the data. When both the predicted values match transitions that are observed in the data, then it is likely that these three transitions are in the progression of  $v''+1$ ,  $v''$ , and  $v''-1$  from a single  $v'$ . Once the  $v''$  and its associated wavelength are known, the entire list of wavelengths corresponding to transitions from some  $v'$  to all the  $v''$  levels, using the known  $v''$  spacing can be calculated. Then, if each of these calculated wavelengths corresponds to an observed transition in the spectra, it can be reasonably well assumed that this list of wavelengths does indeed correspond to the transitions from one level in the excited state ( $v' = \text{const}$ ) to each level of the ground state ( $v''$  goes from 0 up). Then another unknown transition is picked and the whole process is repeated. Eventually, the entire Deslandres table of the  $S_2$  ( $B''-X$ ) system could be generated.

Careful and detailed analysis as described above seems to indicate that the previously unexplained structure of the  $S_2$  molecule is indeed

the  $B''^3\Pi_u^- - X^3\Sigma_g^-$  system which is superimposed on the  $S_2$  (B-X) system. This is the first time that the spectrum of pure sulfur has been seen from a discharge source. The intensities of the entire system are greatly enhanced and the structure is visible in such detail that all the (B-X) system transitions are visible. Perhaps the ( $B''-X$ ) system is so weak that under other conditions it is not readily distinguishable. Tables 3 and 4 are a Deslandres table of the  $S_2$  ( $B''-X$ ) system. At this writing there has not been enough detailed spectral data to give a complete table, but those transitions listed seem to suggest very close agreement between calculated/predicated values and observed transitions. Since only a few of the many  $v''$  levels have been recorded, it is not possible yet to assign a number to these  $v''$  levels. It remains for much more detailed and precise spectra and analysis to reveal the entire structure of the  $S_2$  ( $B''-X$ ) system. With both the (B-X) system and the ( $B''-X$ ) system, virtually every single observed transition appears to be explained. It is unlikely that such close agreement could be obtained if the "unexplained" structure was from some other source.

Table 3. The Deslandres Table of the  $B^3\Pi_u^- - X^3\Sigma_g^-(v'' \leq 10)$ .

$v'$	0	1	2	3	4	5	6	7	8	9	10
	3086.4	3156.7	3229.7	3305.5	3384.2	3466.1	3551.3	3640.0	3732.4	3828.8	3929.4
								3640	3732.6	3828.6	
	3070.0	3139.6	3211.7	3286.7	3364.5	3445.4	3529.6	3617.2	3708.4	3803.6	3902.8
	3070	3140	3212	3286	3364.7	3445	3529.8	3617	3706.4	3805.3	3903
	3016.3	3088.4	3153.0	3225.2	3300.1	3378	3458.8	3542.9	3630.4	3721.5	3816.5
							3459	3542.5	3630.4	3721.6	3816.6
	2977.0	3042.4	3110.1	3180.3	3253.2	3328.7	3407.2	3488.8	3573.6	3661.9	3753.8
		3042	3110	3180	3253	3329	3407	3489		3661.6	
	2910.2	2972.7	3073.3	3104.2	3173.6	3245.4	3320	3397.4	3477.8	3561.3	3648.2
			3073.3						3477.8	3560.9	3650
	2876.2	2937.4	3000.5	3065.8	3133.4	3203.5	3276.1	3351.4	3429.6	3510.8	3595.3
		2937.4	3000				3276	3352		3510.5	
	2808.7	2866.8	2926.9	2989.0	3053.2	3119.7	3188.6	3259.9	3333.8	3410.5	3490.1
						3120	3188.7	3260	3333.5	3410.5	3490

Table 4. The Deslandres Table of the  $B^{-3}\pi_u^{-3}\chi^3\Sigma_g^{-}(v'' \leq 10)$ .

$v''$	11	12	13	14	15	16	17	18	19	20	21
	4034.5	4144.4	4259.4	4379.8	4506.1	4638.7	4778.0	4924.6	5079.1	5241.9	5414
				4379.1	4506	4639.2	4778				
	4006.5	4114.8	4228.2	4346.8	4471.2	4601.7	4738.8	4883	5034.7	5194.7	5363.7
	4007.1	4114.3	4228.9				4738				
	3915.6	4019.0	4127.0	4240	4358.3	4482.2	4612.1	4748.6	4892.0	5042.9	5201.9
	3915.1		4127	4239	4358	4482					
	3849.6	3949.5	4053.8	4162.8	4276.7	4395.9	4520.9	4651.9	4789.4	4934.0	5086.1
	3849.6	3948.9	4053.8	4162.3	4277.2	4396	4520.5				
	3738.6	3832.8	3930.9	4033.3	4140.2	4251.8	4368.6	4490.8	4618.9	4753.2	4894.2
	3736.5	3832.1	3932.9		4139.3	4251.6	4367.6				
	3683.0	3774.4	3869.5	3968.7	4072.1	4180.1	4292.9	4410.8	4534.3	4663.7	4799.4
	3682.3	3774.2	3867.3	3968.4	4073.6	4179.8	4291.5	4410.1	4534.5		
	3572.8	3658.7	3748	3840.9	3937.7	4038.6	4143.8	4253.6	4368.3	4488.3	4613.8
		3659		3841	3938			4253.8	4368	4488	4614

## V. CONCLUSIONS

For the first time, extremely stable, diffuse discharges have been achieved in sulfur. These discharges are self sustaining and can be operated at temperatures from 0°C to 250°C. Using the self heating of the discharge minimizes the amount of external heat needed to operate the discharge.

Using these pure sulfur discharges for spectroscopic studies has allowed the observation of the  $S_2$  emission spectra in great detail with intensities that have not been previously attainable. Because the  $S_2$  spectra is virtually the only spectra that the pure  $S_2$  discharges produce (some weak atomic lines should become observable under high resolution), it could be studied in minute detail. Careful analysis of the spectra in conjunction with already established wavelengths and transition values of the  $S_2$  (B-X) system has allowed accurate determination of the  $X^3\Sigma_g^-$  ground state oscillation frequency and the first three anharmonicity constants. Then, using these constants, all the transitions in the  $S_2$  (B-X) system were calculated. Virtually all the calculated transitions were observed, thus allowing complete identification of the  $S_2$  (B-X) system.

Once the  $S_2$  (B-X) system was characterized to the fourth order, it could be seen that there was still unexplained structure in the observed data. Subsequent evaluation, using the ground state constants and the fact that the  $B^3\Sigma_u^-$  state is perturbed by the  $B'^3\Pi_u^-$  state, prompted investigation into transitions between the  $B'^3\Pi_u^-$  state and the  $X^3\Sigma_g^-$  state. This effort led to the first observation of the  $B'^3\Pi_u^- - X^3\Sigma_g^-$  system and a tentative identification of some of these transitions.

## VI. RECOMMENDATIONS

The  $S_2$  system looks very promising as an electrically pumped laser system. The energy levels are fortuitously placed and the efficiencies seem to be good. The "closed loop" molecular processes of the  $S_2$  molecule indicate that the system should be scalable and capable of high power CW operation. The prospect of making a tunable visible laser on the  $S_2$  molecular transitions should definitely be pursued.

Of course much more work on the identification and characterization of the  $S_2$  (B-X) system is now possible and should be done. There are perhaps other states that disturb the ground state at higher  $v''$  values and there may be some other effects of the overlapping of the  $B''^3\Pi_u^-$  and  $B^3\Sigma_u^-$  states which need to be investigated, and certainly the precision could be improved.

Many more types of studies can now be done on  $S_2$ , using these self-sustained discharges in Sulfur, and the techniques developed to produce them. Some of these might be: 1) further selective excitation studies on other levels of both upper states; 2) electron drift velocity measurements; 3) cross-section determinations; 4) the kinetics of the discharges; 5) accurate determination of the potential energy curves; and 6) as previously mentioned, the  $S_2$  ( $B''$ -X) system can be investigated.

## BIBLIOGRAPHY

1. S. R. Leone and K. G. Kosnik, *Appl. Phys. Lett*, 30, 346 (1977).
2. M. A. Henesian, R. L. Herbst, and R. L. Byer, *J. Appl. Phys.*, 47, 1515 (1975).
3. J. H. Parks, *Appl. Phys. Lett*, 31, 192 (1977).
4. J. H. Parks, *Appl. Phys. Lett*, 31, 297 (1977).
5. J. G. Eden, *Appl. Phys. Lett*, 31, 448 (1977).
6. E. J. Schermitschek, J. E. Cells, and J. A. Triss, *Appl. Phys. Lett*, 31, 608 (1977).
7. K. Y. Tang, R. O. Hunter, Jr., J. Oldenettel, C. Howton, D. Huestis, D. Eckstron, B. Perry, and M. McCusker, *Appl. Phys. Lett*, 32, 266 (1978).
8. A. Fowler and W. M. Verdeja, *Proc. Roy. Soc.*, A132, 310 (1931).
9. G. Lakshminarayana and C. G. Mahajan, *J. Quant. Spectrosc. Radiat., Transfer*, 16, 549 (1976).
10. B. Meyer, Elemental Sulfur (Interscience, New York, 1965), esp. Chap 7.
11. Ref. 10, Chap 5.
12. R. Powell and H. Eyring, *J. Am. Chem. Soc.*, 65, 648 (1943).
13. G. Gee, *Trans, Faraday Soc.*, 48, 513 (1952) and F. Fairbrother, G. Gee, and E. T. Merrall, *J. Polymer Sci*, 61, 459 (1959).
14. A. V. Tobolsky and A. Eisenberg, *J. Am. Chem. Soc.*, 81, 780 (1959).
15. For an excellent discussion of ion-clustering, see E. W. McDaniels, Collision Phenomenon in Ionized Gases; John Wiley & Sons, NY (1964).
16. Ref. 10, Chap 7, J. Berkowitz, "Molecular Composition of Sulfur Vapor".
17. W. H. Evans and D. D. Wagman, *J. Res. Natl. Bur Std (U.S.)*, 49, 141 (1952).
18. W. A. West and A. W. Menzies, *J. Phys. Chem*, 33, 1880 (1929).
19. H. Braune, S. Peter and V. Neveling, *Z. Naturforsch*, 6a, 32 (1951).
20. J. A. Kearnaahan and P.H-L Tang, *Can. J. Phys.*, 53, 1114 (1975).



21. C. E. Moore, Atomic Energy Levels, Vol 1, NBS, Circular 467 (1952).
22. J. M. Ketteringham, PhD thesis (University of Oxford, 1964) (unpublished).
23. S. M. Naude, Ann. Phys. (Leips), 3, 201 (1943).
24. J. M. Ricks and R. F. Barrow, Can. J. Phys., 47, 2423 (1969).
25. K. A. Meyer and D. R. Crosley, J. Chem. Phys., 59, 3153 (1973).
26. T. H. McGee and R. E. Weston, Jr., Chem. Phys. Lett, 47, 352 (1977).
27. M. J. Seaton, Proc. of the Phys. Soc., London, 79, 1105 (1962).
28. R. W. B. Pearse and A. G. Gaydon, The Identification of Molecular Spectra (Chapman & Hall, Ltd., London, 1965).
29. B. Rosen, Selected Constants - Spectroscopic Data Relative to Diatomic Molecules (Pergamon, Oxford, 1970).
30. A. Christy and S. M. Naude, Physical Review, 37, 903, (1931).
31. American Institute of Physics Handbook, 3rd edition, McGraw-Hill Book Company, (1972).
32. Simons, Parr, and Finlay, J. Chem. Phys., 59, 3229 (1973).

## APPENDIX A

### PROGRESSIVE HISTORY of the DISCHARGE TUBES

There were 6 discharge tubes and 1 absorption tube constructed. The progression or development of the final configuration is outlined below.

#### Tube #1

1. Electrodes: tungsten - not reversed\*
2. Sulfur: not distilled\*\*
3. Tube: 7 mm dia x 12 $\frac{1}{2}$ " discharge area.
4. Run Time:  $\approx$  10 min. total time.

A low pressure discharge which ran in the furnace for a short time only. The tube flashes at breakdown, but the current runs away. Apparently the discharge generates its own heat. Heating/arcing produced a hole in the cathode end.

#### Tube #2

1. Electrodes: Tungsten - not reversed
2. Sulfur: not distilled
3. Tube: 12" x 7 mm dia discharge area with external sidearm.
4. Run Time:  $\approx$  1 hour

Operated with the entire discharge area including electrodes inside the furnace. The VP was supposed to be maintained at a desired level by controlling the temperature in the sidearm. Only low pressure discharges

---

\*Reversing refers to the particular method of constructing the electrodes. A "reversed" one is where there are larger electrodes and greater spacing between the electrodes and the tube walls.

\*\*The distillation process is described in Section III of the thesis.

were observed. The cathode was broken accidentally, but the tube may also have had a hole poked in the quartz by the high voltage.

Tube #3

1. Electrodes: anode - tungsten  
cathode - Hastelloy  
reversed, because a new type of flash lamp was used.
2. Sulfur: not distilled
3. Tube: 7 mm x 15" discharge area with external sidearm
4. Run Time: 3 hours
5. Operation: Inside furnace/In open air

The tube would discharge, overpressure and extinguish while in the furnace. Outside, it ran at 300°C+ and the cathode got so hot that after 2.5 hours continuous operation (when shut off) the G.E. 1 seal broke. The cathode was glowing red hot when turned off.

Tube #4

1. Electrodes: Hastelloy - reversed
2. Sulfur: not distilled
3. Tube: 11 mm dia x 10½" with/without sidearm
4. Run time: 1 to 2 hours
5. Operation: In the open, with heated sidearm

This tube operated so erratically that it is hard to say if it was overpressuring or the sulfur had been consumed. There was no visible sulfur in the tube when it ceased operation and a He leak check showed the tube to be tight.

Tube #4

1. Electrodes: Hastelloy - reversed
2. Sulfur: distilled
3. Tube: same as 4(a), but this tube was baked prior to sealing

4. Run time: 3 hours

5. Operation: a) Free standing with heated sidearm.  
b) Free standing (no sidearm) heated anode end.

Many new techniques were initiated with this tube. It was filled with distilled sulfur, eventually the sidearm removed, and although free standing, would run with external heating of the anode end.

Tube 4 (c) & (d)

This is the same tube as 4(b) but it has been inserted in the heat shield for temperature control. The only difference between (c) and (d) is that (d) has the quartz observation window added to the pyrex shield.

4. Run time: 15 hours

5. Operation: shielded

After 18 hours the tube extinguished and would not discharge again. The sulfur had apparently been consumed. This tube's discharge was fully controllable using the shield and external heat. The tube broke in the ultrasonic cleaner while being cleaned for refilling.

Tube #5

1. Electrodes: Hastelloy - reversed
2. Sulfur: distilled
3. Tube: 8 mm dia x 10 $\frac{1}{2}$ " discharge area
4. Run time: 33.5 hours CW and 8.5 hours pulsed (still operational)
5. Operation: shielded

This tube was the mainstay of the operation. Almost all spectra (using sulfur only) were made with this tube. It's electrodes corroded badly but there is still some sulfur visible, and the tube is still operable. The stable discharge can be completely controlled.

Tube #6

1. Electrodes: Hastelloy - reversed
2. Sulfur: distilled
3. Tube: 8 mm dia x  $9\frac{1}{2}$ " discharge area
4. Run time: 38 hours CW and 5.5 hours pulsed (still operable)
5. Operation: shielded
6. Helium filled

This tube was used for all the S-HE spectra, and also has a very stable discharge which is easily and fully controllable.

Tube #7

1. Electrodes: none
2. Sulfur: distilled
3. Tube:  $1\frac{1}{4}$ " dia x 11" cylinder
4. Run time: N/A

This tube was not a discharge tube. It was only a quartz cylinder filled with sulfur that was used in the absorption measurements. It was heated as high as  $1200^{\circ}\text{C}$ .

## APPENDIX B

### SULFURATION OF VARIOUS METALS

The indications that Hastelloy is better at resisting  $S_2$  attack was substantially born out by a small scale sulfidation test carried out in the metals laboratory. Several samples of Al, Hastelloy 304 & 410 stainless steel, and mild steel were placed in a sulfur environment at a temperature of  $600^{\circ}C$  for one (1) hour.

The samples were tared prior to the experiment and weighed again afterwards. The Hastelloy gained .2%, the Aluminum gained .0079%, the mild steel lost 1.8%, and the stainless steels lost .04% and .06%, respectively. This test was a "static" test and only indicates a passive attack on the material. As an electrode, it would be under bombardment by ions and electrons as well as heat and the sulfur.

## APPENDIX C

### MATERIAL ANALYSIS

An electron microscope was used to determine the elemental constituents of various deposits. Many of the early tube failures were analyzed by learning the nature of the deposits on the electrodes and walls of the tubes. The electrodes of the early tubes were the tungsten electrodes of the xenon flashlamps, but they were so severely attacked that in at least one case caused failure of the tube.

The decision was made to look for a more resistant electrode material which eventually led to the determination to use Hastelloy. Alluminum was tried, but failed during tube assembly because of the glass-blowing heat.

Switching to Hastelloy necessitated reversing the feed-throughs and also resulted in a larger diameter tube at the electrode ends. This gave more room between the electrodes and walls, which also aided in reducing the stress on the quartz from the hot cathode. It was often observed that the cathode would run red hot during the discharge. Adding He helped because it conducted the heat away from the cathode and also because it absorbed energy from the  $S_2$  ions through collisions prior to contacting the cathode surface.

The anode often developed crusty deposits but was not severely attacked and only minor sputtering of material was noticed.

The constituents of Hastelloy are (by % weight)

Mn	-	.1
Si	-	1
Cr	-	15.5
Co	-	2.5

Mo	-	16.0
W	-	3.8
Fe	-	5.5
Ni	-	balance

All of these materials form stable sulfides. When the Hastelloy was attacked by the  $S_2$  vapors, the surface would flake off and deposits would form on the walls. The flakes were analyzed and found to contain Cr, Fe, Ni, and Sulfur, and the deposits on the glass contained Cr, Fe, Ni, W, Mo, and Sulfur. The cathode itself showed considerable Sulfur injected into the surface with much higher concentrations in the flaked-off areas.

Analysis of the various cold traps deposits, and the deposits left when backing out the tubes, gave mostly the contaminants that would be expected from the glass, but often gave some silver and occasionally some exotic substance like Cadmium, Paladium or Atimony.



VITA

Drew A. Peterson was born on 8 December 1945 in Salina, Utah. He graduated from high school in Salt Lake City, Utah in 1965 and attended the University of Utah from which he received the degree of Bachelor of Science in Physics in December 1970. Upon graduation, he received a commission in the USAF through the ROTC program. He completed pilot training and received his wings in June 1972. He then served as a KC-135 pilot in the 92 Bomb Wing at Fairchild AFB, Washington until entering the School of Engineering, Air Force Institute of Technology, in June 1978.

Permanent address: 2210 Creek Road  
Sandy, Utah 84070

UNCLASSIFIED

SECURITY CLASSIFICATION OF THIS PAGE (When Data Entered)

REPORT DOCUMENTATION PAGE		READ INSTRUCTIONS BEFORE COMPLETING FORM
1. REPORT NUMBER AFIT/GEP/PH/78D-10	2. GOVT ACCESSION NO.	3. RECIPIENT'S CATALOG NUMBER
4. TITLE (and Subtitle)  PURE SULFUR DISCHARGES AND ASSOCIATED SPECTRA		5. TYPE OF REPORT & PERIOD COVERED  MS Thesis
		6. PERFORMING ORG. REPORT NUMBER
7. AUTHOR(s)  Drew A. Peterson Capt		8. CONTRACT OR GRANT NUMBER(s)
9. PERFORMING ORGANIZATION NAME AND ADDRESS  Air Force Institute of Technology (AFIT/EN) Wright-Patterson AFB OH 45433		10. PROGRAM ELEMENT, PROJECT, TASK AREA & WORK UNIT NUMBERS
11. CONTROLLING OFFICE NAME AND ADDRESS  Air Force Weapons Lab/ALE Kirtland AFB NM 87117		12. REPORT DATE October 1978
		13. NUMBER OF PAGES 55
14. MONITORING AGENCY NAME & ADDRESS (if different from Controlling Office)		15. SECURITY CLASS. (of this report)  Unclassified
		15a. DECLASSIFICATION/DOWNGRADING SCHEDULE
16. DISTRIBUTION STATEMENT (of this Report)  Approved for public release; distribution unlimited		
17. DISTRIBUTION STATEMENT (of the abstract entered in Block 20, if different from Report)		
18. SUPPLEMENTARY NOTES		Approved for public release; IAW AFR 190-17  J. P. HIPPS, Major, USAF Director of Information 19 Jan 79
19. KEY WORDS (Continue on reverse side if necessary and identify by block number)  Sulfur Discharges Sulfur Spectra		
20. ABSTRACT (Continue on reverse side if necessary and identify by block number)  Stable, glow discharges in pure sulfur and He-sulfur have been achieved for the first time, at operating temperatures between 0°C and 250°C. This result indicates that $S_2^+$ is broken directly into $S_2^+$ and means that temperatures much less than 600°C can be used. The $S_2^+(B-X)$ band emission is observed in great detail, and through analysis of these spectra the ground electronic state constants have been determined to the fourth order. The first observation of the $B11\ 3\pi_u^- - X^3\Sigma_g^-$ system transitions is made, and tentatively identified.		

DD FORM 1 JAN 73 1473

EDITION OF 1 NOV 65 IS OBSOLETE

79 01 20 161 UNCLASSIFIED

SECURITY CLASSIFICATION OF THIS PAGE (When Data Entered)

UNCLASSIFIED

SECURITY CLASSIFICATION OF THIS PAGE(When Data Entered)

Only S<sub>2</sub> band emission is observed and no atomic lines were observable.

UNCLASSIFIED

SECURITY CLASSIFICATION OF THIS PAGE(When Data Entered)